

A Lightweight RL-Driven Deep Unfolding Network for Robust WMMSE Precoding in Massive MU-MIMO-OFDM Systems

Kexuan Wang and An Liu, *Senior Member, IEEE*

Abstract—Weighted Minimum Mean Square Error (WMMSE) precoding is widely recognized for its near-optimal weighted sum rate performance. However, its practical deployment in massive multi-user (MU) multiple-input multiple-output (MIMO) orthogonal frequency-division multiplexing (OFDM) systems is hindered by the assumption of perfect channel state information (CSI) and high computational complexity. To address these issues, we first develop a wideband stochastic WMMSE (SWMMSE) algorithm that iteratively maximizes the ergodic weighted sum-rate (EWSR) under imperfect CSI. Building on this, we propose a lightweight reinforcement learning (RL)-driven deep unfolding (DU) network (RLDDU-Net), where each SWMMSE iteration is mapped to a network layer. Specifically, its DU module integrates approximation techniques and leverages beam-domain sparsity as well as frequency-domain subcarrier correlation, significantly accelerating convergence and reducing computational overhead. Furthermore, the RL module adaptively adjusts the network depth and generates compensation matrices to mitigate approximation errors. Simulation results under imperfect CSI demonstrate that RLDDU-Net outperforms existing baselines in EWSR performance while offering superior computational and convergence efficiency.

Index Terms—WMMSE, imperfect CSI, deep-unfolding, DRL.

I. INTRODUCTION

The 6G wireless communication adopts massive multi-user (MU) multiple-input multiple-output (MIMO) and orthogonal frequency-division multiplexing (OFDM) technologies to support rapid data growth. Weighted Minimum Mean Square Error (WMMSE) precoding has been widely recognized for enabling near-optimal weighted sum-rate performance [1]. However, the practical deployment of WMMSE in massive MU-MIMO-OFDM faces two critical challenges [2]. First, it heavily relies on accurate channel state information (CSI), which is often unavailable due to limited pilot resources and channel aging. Second, its high computational complexity must be reduced to meet latency and deployment constraints.

To address the first challenge, [3]–[5] modeled imperfect CSI using Gaussian-distributed posterior channel models and formulated the robust precoding problem as an ergodic weighted sum-rate (EWSR) maximization problem under a sum power constraint (SPC). Specifically, [3] and [4] developed stochastic WMMSE (SWMMSE) based on the sample average approximation (SAA) method, which alternately optimizes the receiver, weighting, and precoding matrices using virtual CSI samples drawn from channel error statistics. [5] iteratively computed deterministic equivalents of the EWSR and optimized the precoders via the majorization-minimization

(MM) method. However, these methods either incur high per-iteration complexity scaling cubically with the number of transmit antennas or suffer from slow convergence due to nested iterations. To address the second challenge, some robust linear precoding schemes, such as regularized zero-forcing (RZF) [6] and signal-to-leakage-and-noise ratio (SLNR) precoding [7], have been proposed but generally deliver sub-optimal performance compared to WMMSE-based methods because they do not directly optimize the EWSR objective [5]. Data-driven approaches such as [8] and [9] employed multi-layer perceptrons (MLPs) and convolutional neural networks (CNNs) to approximate the WMMSE algorithm, but suffer from limited interpretability and generalization. More recently, [2] proposed a practical WMMSE network (PO-WMMSE Net) that combines deep unfolding and approximation techniques to reduce complexity and accelerate convergence. By leveraging domain knowledge and introducing only a small number of trainable compensation matrices, it achieves stable performance across diverse scenarios. Nevertheless, it employs fixed compensation matrices and a uniform network depth for all channel conditions, limiting its flexibility under highly dynamic CSI. Moreover, all the aforementioned methods are designed for narrowband systems. When extended to wideband systems, they must be applied independently to each subcarrier, resulting in prohibitive computational overhead.

To address these challenges, this paper first develops a wideband variant of the SWMMSE algorithm [3] and then enhances it into a practical-oriented, lightweight reinforcement learning-driven deep-unfolding network (RLDDU-Net). Specifically, RLDDU-Net consists of a deep-unfolding (DU) module and a reinforcement learning (RL) module. The DU module maps each iteration of the wideband robust WMMSE into a network layer and applies approximation techniques to significantly reduce computational complexity by leveraging beam-domain sparsity and subcarrier correlation. These approximations also enable the direct use of CSI statistics, avoiding the sample average approximation (SAA) and nested iterations required in conventional robust WMMSE methods, thereby accelerating convergence. The RL module adaptively generates compensation matrices to mitigate approximation errors and adjusts the network depth in response to varying CSI conditions. Numerical results under imperfect CSI demonstrate that the proposed RLDDU-Net significantly outperforms baseline approaches.

II. SYSTEM MODEL AND PROBLEM FORMULATION

As illustrated in Fig. 1, we consider a massive MU-MIMO-OFDM system operating in time-division duplexing (TDD)

Kexuan Wang and An Liu are with the College of Information Science and Electronic Engineering, Zhejiang University, Hangzhou 310027, China (email: {kexuanWang, anliu}@zju.edu.cn). (*Corresponding Author: An Liu*)

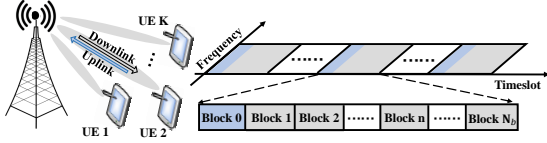


Figure 1. System model and time slot diagram

mode, where a base station (BS) with a uniform planar array (UPA) of M_t -antennas serves K users, each with M_r -antennas ($M_r \ll M_t$). Specifically, the time domain is divided into multiple timeslots, each further split into $(N_b + 1)$ blocks: the 0-th block is used for uplink training, and the remaining N_b blocks are reserved for downlink transmission. In the frequency domain, subcarriers are grouped into resource blocks (RBs), each consisting of 12 consecutive subcarriers. In 5G systems, adjacent N_{RB} RBs (typically $N_{RB} = 4$) are grouped into a resource block group (RBG), which serves as the granularity for precoding to reduce computational overhead [10]. We assume block flat fading per subcarrier, i.e., the channel remains constant within each block. In the following, we consider one timeslot and one RBG as an example.

During the uplink training phase (i.e., the 0-th block), advanced Bayesian estimation methods exploit beam-domain sparsity to obtain posterior channel estimates with low pilot overhead [11]. The posterior beam-domain channel at subcarrier f is modeled as $\mathbf{H}_{k,f,0}^b \sim \mathcal{CN}(\bar{\mathbf{H}}_{k,f,0}^b, \Delta \mathbf{H}_{k,f,0}^b)$, where $\bar{\mathbf{H}}_{k,f,0}^b \in \mathbb{C}^{M_r \times M_t}$ and $\Delta \mathbf{H}_{k,f,0}^b \in \mathbb{C}^{M_r \times M_t}$ are the posterior mean and covariance. For any downlink block n ($n = 1, \dots, N_b$), the estimated beam-domain channel at subcarrier f is denoted as $\mathbf{H}_{k,f,n}^b \in \mathbb{C}^{M_r \times M_t}$. To capture channel aging, channel evolution across blocks is modeled using a first-order Gauss-Markov process [5] as:

$$\mathbf{H}_{k,f,n}^b = \beta_{k,f,n} \bar{\mathbf{H}}_{k,f,0}^b + \sqrt{1 - \beta_{k,f,n}^2} \mathbf{M}_{k,f} \odot \mathbf{W}_{k,f,n}, \forall k, n,$$

where \odot denotes the element-wise multiplication, $\mathbf{M}_{k,f} \in \mathbb{C}^{M_r \times M_t}$ is a non-negative matrix representing the amplitude profile, and $\mathbf{W}_{k,f,n} \in \mathbb{C}^{M_r \times M_t}$ is an i.i.d complex Gaussian noise matrix with zero mean and unit variance entries. The value of $\beta_{k,f,n} \in (0, 1)$ and $\mathbf{\Omega}_{k,f} \triangleq \mathbf{M}_{k,f} \odot \mathbf{M}_{k,f}$ can be acquired through the sounding process at the BS. Accordingly, the distribution of $\mathbf{H}_{k,f,n}^b$ is derived as

$$\mathbf{H}_{k,f,n}^b \sim \mathcal{CN}(\bar{\mathbf{H}}_{k,f,n}^b, \Delta \mathbf{H}_{k,f,n}^b) \quad (1)$$

where $\Delta \mathbf{H}_{k,f,n}^b = \beta_{k,f,n}^2 \Delta \mathbf{H}_{k,f,0}^b + (1 - \beta_{k,f,n}^2) \mathbf{\Omega}_{k,f}$, and $\bar{\mathbf{H}}_{k,f,n}^b = \beta_{k,f,n} \bar{\mathbf{H}}_{k,f,0}^b$. Without loss of generality, this paper assumes that $\{\Delta \mathbf{H}_{k,f,n}^b, \bar{\mathbf{H}}_{k,f,n}^b, \forall k, f, n\}$ are known and uses them to design the robust precoders.

In the downlink transmission block n ($n \geq 1$), the BS applies an antenna-domain precoder $\mathbf{V}_{k,n} \in \mathbb{C}^{M_t \times M_r}$ for each user k to process the transmit signal $\mathbf{s}_{k,f,n} \in \mathbb{C}^{M_r \times 1}$, where $\mathbb{E}[\mathbf{s}_{k,f,n} \mathbf{s}_{k,f,n}^H] = \mathbf{I}$. For simplicity, the block index n is omitted in the following when no ambiguity arises. The antenna-domain channel at subcarrier f is expressed as $\mathbf{H}_{k,f} = \mathbf{H}_{k,f}^b \mathbf{\Phi}$, where $\mathbf{\Phi} \in \mathbb{C}^{M_t \times M_t}$ is the array response matrix, modeled as a normalized discrete Fourier transform matrix that satisfies $\mathbf{\Phi} \mathbf{\Phi}^H = \mathbf{I}$ for large-scale uniform planar arrays. The received signal at user k and subcarrier f is

$$\mathbf{y}_{k,f} = \mathbf{H}_{k,f} \mathbf{V}_k \mathbf{s}_{k,f} + \sum_{m \in \mathcal{K}/\{k\}} \mathbf{H}_{k,f} \mathbf{V}_m \mathbf{s}_{m,f} + \mathbf{n}_{k,f},$$

where $\mathbf{n}_{k,f} \sim \mathcal{CN}(\mathbf{0}, \sigma_k^2 \mathbf{I})$ denotes additive white Gaussian noise, and $\mathcal{K} \triangleq \{1, 2, \dots, K\}$ is the set of all user indices. The achievable transmission rate of user k at subcarrier f is

$$\mathcal{R}_{k,f}(\mathbf{V}_k) = \log \det \left(\mathbf{I} + \frac{\mathbf{H}_{k,f} \mathbf{V}_k \mathbf{V}_k^H \mathbf{H}_{k,f}^H}{\sum_{m \in \mathcal{K}/\{k\}} \mathbf{H}_{k,f} \mathbf{V}_m \mathbf{V}_m^H \mathbf{H}_{k,f}^H + \sigma_k^2 \mathbf{I}} \right).$$

To enhance system performance under imperfect CSI, the robust precoding problem is formulated as the following EWSR maximization problem subject to a SPC:

$$\begin{aligned} \mathbf{P}_1 : \max_{\mathbf{V}} & \sum_{k \in \mathcal{K}} \sum_{f \in \mathcal{F}} \omega_k \mathbb{E}[\mathcal{R}_{k,f}(\mathbf{V}_k^i)], \\ \text{s.t.} & \sum_{k \in \mathcal{K}} \text{Tr}(\mathbf{V}_k \mathbf{V}_k^H) \leq P_{max}. \end{aligned}$$

where $\mathcal{F} \triangleq \{1, 2, \dots, 12N\}$ is the set of subcarrier indices, ω_k represents the priority of user k , and \mathbb{E} is the expectation taken over distributions (1).

III. ROBUST PRECODING ALGORITHM AND NETWORK DESIGN

A. A Wideband Variant of SWMMSE Algorithm

We first develops a wideband variant of the SWMMSE in [3] to solve \mathbf{P}_1 . To avoid directly handling the constraint, we incorporate it into the objective and consider problem \mathbf{P}_2 :

$$\mathbf{P}_2 : \max_{\mathbf{V}} \sum_{k \in \mathcal{K}} \sum_{f \in \mathcal{F}} \omega_k \mathbb{E}[\tilde{\mathcal{R}}_{k,f}],$$

where

$$\begin{aligned} \tilde{\mathcal{R}}_{k,f} = \log \det & \left(\mathbf{I} + \mathbf{H}_{k,f} \mathbf{V}_k \mathbf{V}_k^H \mathbf{H}_{k,f}^H \left(\sum_{m \in \mathcal{K}/\{k\}} \mathbf{H}_{k,f} \mathbf{V}_m \right. \right. \\ & \left. \left. \times \mathbf{V}_m^H \mathbf{H}_{k,f}^H + \frac{\sigma_k^2}{P_{max}} \sum_{m=1}^K \text{Tr}(\mathbf{V}_m \mathbf{V}_m^H \mathbf{I}) \right)^{-1} \right). \quad (2) \end{aligned}$$

According to [2], any stationary point \mathbf{V}_k^{**} of \mathbf{P}_1 corresponds to a stationary point \mathbf{V}_k^* of \mathbf{P}_2 , satisfying $\mathbf{V}_k^{**} = \xi \mathbf{V}_k^*$ with $\xi = \sqrt{P_{max}} (\sum_{k=1}^K \text{Tr}(\mathbf{V}_k^* (\mathbf{V}_k^*)^H))^{-\frac{1}{2}}$. Therefore, \mathbf{P}_1 can be solved by addressing \mathbf{P}_2 , followed by a scaling operation.

Then, according to [3, Lemma 1], \mathbf{P}_2 can be equivalently reformulated as the following weighted MMSE problem \mathbf{P}_3 by introducing auxiliary variables $\{\mathbf{U}_{k,f}, \mathbf{W}_{k,f}\}$:

$$\mathbf{P}_3 : \min_{\mathbf{V}} \mathbb{E} \left[\min_{\{\mathbf{U}, \mathbf{W}\}} \sum_{k \in \mathcal{K}} \sum_{f \in \mathcal{F}} \omega_k \left(\text{Tr}(\mathbf{W}_{k,f} \tilde{\mathbf{E}}_{k,f}) - \log \det \mathbf{W}_{k,f} \right) \right],$$

where the MSE matrix $\tilde{\mathbf{E}}_{k,f}$ is given by

$$\begin{aligned} \tilde{\mathbf{E}}_{k,f} \triangleq & (\mathbf{I} - \mathbf{U}_{k,f}^H \mathbf{H}_{k,f} \mathbf{V}_k) (\mathbf{I} - \mathbf{U}_{k,f}^H \mathbf{H}_{k,f} \mathbf{V}_k)^H \\ & + \sum_{m \in \mathcal{K}/\{k\}} \mathbf{U}_{k,f}^H \mathbf{H}_{k,f} \mathbf{V}_m \mathbf{V}_m^H \mathbf{H}_{k,f}^H \mathbf{U}_{k,f} + \sigma_k^2 \mathbf{U}_{k,f}^H \mathbf{U}_{k,f}. \end{aligned}$$

Noting that fixing any two of \mathbf{U} , \mathbf{W} , and \mathbf{V} transforms \mathbf{P}_3 into a convex problem with a closed-form solution, we solve \mathbf{P}_3 using the block coordinate descent method [1]. Specifically, at the i -th iteration, given \mathbf{V}^{i-1} , the optimal \mathbf{U}^i is

$$\mathbf{U}_{k,f}^i = (\mathbf{A}_{k,f}^i)^{-1} \mathbf{H}_{k,f} \mathbf{V}_k^{i-1}, \forall k, f, \quad (3)$$

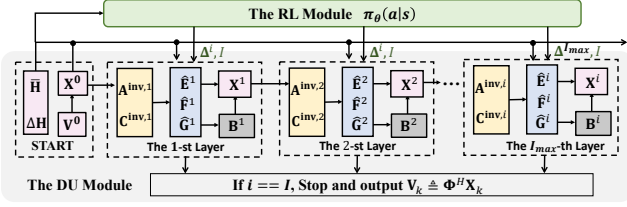


Figure 2. The RLDDU-Net Architecture.

where the variable $\mathbf{A}_{k,f}^i = \sum_{m=1}^K \mathbf{H}_{k,f} \mathbf{V}_m^{i-1} (\mathbf{V}_m^{i-1})^H \mathbf{H}_{k,f}^H + \frac{\sigma_k^2}{P_{max}} \sum_{m=1}^K \text{Tr}(\mathbf{V}_m^{i-1} (\mathbf{V}_m^{i-1})^H) \mathbf{I}$. Once \mathbf{U}^i is further fixed, the optimal weight matrix \mathbf{W}^i is

$$\mathbf{W}_{k,f}^i = (\mathbf{I} - (\mathbf{U}_{k,f}^i)^H \mathbf{H}_{k,f} \mathbf{V}_k)^{-1}, \forall k, f. \quad (4)$$

Finally, setting the derivative of the objective function of \mathbf{P}_2 with respect to \mathbf{V}_k to zero yields the optimal precoder

$$\mathbf{V}_k^i = (\mathbf{B}^i)^{-1} \sum_{f \in \mathcal{F}} \mathbb{E}[\mathbf{H}_{k,f}^H \mathbf{U}_{k,f}^i \mathbf{W}_{k,f}^i], \forall k, \quad (5)$$

where $\mathbf{B}^i = \sum_{f=1}^{12N} \sum_{m=1}^K \mathbb{E}[\frac{\sigma_m^2}{P_{max}} \text{Tr}(\omega_m \mathbf{U}_{m,f}^i \mathbf{W}_{m,f}^i \mathbf{U}_{m,f}^i)^H] \mathbf{I} + \omega_m \mathbf{H}_{m,f}^H \mathbf{U}_{m,f}^i \mathbf{W}_{m,f}^i \mathbf{U}_{m,f}^i \mathbf{H}_{m,f}^H]$. Finally, we calculate (3)-(5) using the SAA method in [3], i.e., sample a virtual channel realization from the distribution (1) to estimate the value of (3)-(5). Following the similar theoretical analysis in [3], it can be proven that it converges to a stationary point of \mathbf{P}_1 .

B. Lightweight RL-Driven Deep-Unfolding Network

Building on wideband SWMMSE, we further propose a lightweight RLDDU-Net, comprising a DU module and a RL module, as shown in Fig. 2. The DU module employs approximation techniques for fast convergence and low complexity, while the RL module uses a policy π_θ to adaptively generate compensation matrices and determine the unfolding depth. We now present the design details.

1) *The DU Module* : In this module, each wideband SWMMSE iteration is first modified and then mapped into a corresponding network layer. Specifically, to better exploit beam-domain sparsity, the deep-unfolding module focuses on optimizing the beam-domain precoders $\{\mathbf{X}_k \triangleq \Phi \mathbf{V}_k, \forall k\}$ instead of $\{\mathbf{V}_k, \forall k\}$. By substituting (3) and (4) into (5) and applying the matrix inversion lemma [12], we obtain that

$$\mathbf{X}_k^i = (\tilde{\mathbf{B}}^i)^{-1} \sum_{f \in \mathcal{F}} \mathbf{E}_{k,f}^i, \quad (6)$$

where $\tilde{\mathbf{B}}^i = \sum_{f=1}^{N_f} \sum_{m=1}^K \frac{\sigma_m^2}{P_{max}} \text{Tr}(\mathbf{F}_{m,f}^i) \mathbf{I} + \mathbf{G}_{m,f}^i$. By defining $\mathbf{D}_{k,f}^i = \mathbf{H}_{k,f}^b \mathbf{X}_k^{i-1} (\mathbf{X}_k^{i-1})^H (\mathbf{H}_{k,f}^b)^H$ and $\mathbf{C}_{k,f}^i = \mathbf{A}_{k,f}^i - \mathbf{D}_{k,f}^i$, the terms $\{\mathbf{E}_{k,f}^i, \mathbf{F}_{k,f}^i, \mathbf{G}_{k,f}^i\}$ are given by

$$\mathbf{E}_{k,f}^i = \mathbb{E}[(\mathbf{H}_{k,f}^b)^H (\mathbf{C}_{k,f}^i)^{-1} \mathbf{H}_{k,f}^b] \mathbf{X}_k^{i-1}, \quad (7)$$

$$\mathbf{F}_{k,f}^i = \mathbb{E}[(\mathbf{C}_{k,f}^i)^{-1} \mathbf{D}_{k,f}^i (\mathbf{A}_{k,f}^i)^{-1}], \quad (8)$$

$$\mathbf{G}_{k,f}^i = \mathbb{E}[(\mathbf{H}_{k,f}^b)^H (\mathbf{C}_{k,f}^i)^{-1} \mathbf{D}_{k,f}^i (\mathbf{A}_{k,f}^i)^{-1} \mathbf{H}_{k,f}^b]. \quad (9)$$

Note that the precoders $\{\mathbf{X}_k^i, \forall k\}$ are fully determined by the three expectation terms $\{\mathbf{E}_{k,f}^i, \mathbf{F}_{k,f}^i, \mathbf{G}_{k,f}^i\}$, which, however, lack closed-form expressions. Although these terms can also be estimated via the SAA method, its convergence is slow and

requires numerous channel realizations under high uncertainty (e.g., large $\Delta \mathbf{H}_{k,f,n}^b$), resulting in high computational cost. To improve efficiency, we derive closed-form approximations for $\{\mathbf{E}_{k,f}^i, \mathbf{F}_{k,f}^i, \mathbf{G}_{k,f}^i\}$ based on the statistical information $\bar{\mathbf{H}}_{k,f,n}^b$ and $\Delta \mathbf{H}_{k,f,n}^b$, as detailed below.

Considering that $\mathbf{A}_{k,f}^i$ and $\mathbf{C}_{k,f}^i$ tend to be diagonal when $M_t \gg M_r$, we approximate $\mathbb{E}[(\mathbf{A}_{k,f}^i)^{-1}]$ and $\mathbb{E}[(\mathbf{C}_{k,f}^i)^{-1}]$ by $\mathbf{A}_{k,f}^{\text{inv},i} + \mathbf{Z}_{k,f}^{\mathbf{A},i}$ and $\mathbf{C}_{k,f}^{\text{inv},i} + \mathbf{Z}_{k,f}^{\mathbf{C},i}$, respectively. Here, $\mathbf{A}_{k,f}^{\text{inv},i}$ and $\mathbf{C}_{k,f}^{\text{inv},i}$ are first-order diagonal Taylor approximations for $\mathbb{E}[(\mathbf{A}_{k,f}^i)^{-1}]$ and $\mathbb{E}[(\mathbf{C}_{k,f}^i)^{-1}]$, given by:

$$\mathbf{A}_{k,f}^{\text{inv},i} = 2\mathbb{E}[\mathbf{A}_{k,f}^i]^+ - \mathbb{E}[\mathbf{A}_{k,f}^i]^+ \mathbb{E}[\mathbf{A}_{k,f}^i] \mathbb{E}[\mathbf{A}_{k,f}^i]^+, \quad (10)$$

$$\mathbf{C}_{k,f}^{\text{inv},i} = 2\mathbb{E}[\mathbf{C}_{k,f}^i]^+ - \mathbb{E}[\mathbf{C}_{k,f}^i]^+ \mathbb{E}[\mathbf{C}_{k,f}^i] \mathbb{E}[\mathbf{C}_{k,f}^i]^+, \quad (11)$$

where \mathbf{Y}^+ denotes the element-wise reciprocal of \mathbf{Y} diagonal entries with off-diagonal elements set to zero, and compensation matrices $\{\mathbf{Z}_{k,f}^{\mathbf{A},i}, \mathbf{Z}_{k,f}^{\mathbf{C},i}\}$ are introduced to narrow the gap between $\{\mathbf{A}_{k,f}^{\text{inv},i}, \mathbf{C}_{k,f}^{\text{inv},i}\}$ and $\{\mathbb{E}[(\mathbf{A}_{k,f}^i)^{-1}], \mathbb{E}[(\mathbf{C}_{k,f}^i)^{-1}]\}$. Then, using compensation matrices $\{\mathbf{O}_{k,f}^{\mathbf{E},i}, \mathbf{O}_{k,f}^{\mathbf{F},i}, \mathbf{O}_{k,f}^{\mathbf{G},i}\}$ to replace trivial cross-related terms, the expectation terms (7)-(9) are approximated as:

$$\hat{\mathbf{E}}_{k,f}^i = \mathbb{E}[(\mathbf{H}_{k,f}^b)^H (\mathbf{C}_{k,f}^{\text{inv},i} + \mathbf{O}_{k,f}^{\mathbf{E},i}) \mathbf{H}_{k,f}^b] \mathbf{X}_k^{i-1}, \quad (12)$$

$$\hat{\mathbf{F}}_{k,f}^i = \mathbf{C}_{k,f}^{\text{inv},i} \mathbb{E}[\mathbf{D}_{k,f}^i] \mathbf{A}_{k,f}^{\text{inv},i} + \mathbf{O}_{k,f}^{\mathbf{F},i}, \quad (13)$$

$$\hat{\mathbf{G}}_{k,f}^i = \mathbb{E}[(\mathbf{H}_{k,f}^b)^H (\hat{\mathbf{F}}_{k,f}^i + \mathbf{O}_{k,f}^{\mathbf{G},i}) \mathbf{H}_{k,f}^b]. \quad (14)$$

The the compensation matrix set $\Delta^i = \{\mathbf{Z}_{k,f}^{\mathbf{A},i}, \mathbf{Z}_{k,f}^{\mathbf{C},i}, \mathbf{O}_{k,f}^{\mathbf{E},i}, \mathbf{O}_{k,f}^{\mathbf{F},i}, \mathbf{O}_{k,f}^{\mathbf{G},i}, \forall k, f\}$ is generated by the RL module detailed in section III-B2. All second-order expectations involved in equations (10)-(9) admit closed-form expressions, as detailed in our prior work [2].

Note that both $\bar{\mathbf{H}}_{k,f,n}^b$ and $\Delta \mathbf{H}_{k,f,n}^b$ exhibit sparse structures, with dominant energy concentrated in $B \ll M_t$ columns. By zeroing negligible entries in $\bar{\mathbf{H}}_{k,f,n}^b$ and $\Delta \mathbf{H}_{k,f,n}^b$, the matrix multiplication complexity in RLDDU-Net is reduced to $O(B^2)$, compared to $O(M_t^2)$ in WMMSE/WR-WMMSE. Similarly, the matrix $\tilde{\mathbf{B}}^i$ has dominant energy along the diagonal and in only $q < M_t$ rows/columns, allowing its inversion to be computed with complexity $O(q^3 + M_t)$, compared to the cost of $O(M_t^3)$ for computing $(\mathbf{B}^i)^{-1}$ in WMMSE/WR-WMMSE. Moreover, to further reduce computational cost by exploiting the strong correlation across adjacent subcarriers, we uniformly sample a subset $\tilde{\mathcal{F}} \in \mathcal{F}$ and compute $\{\hat{\mathbf{E}}_{k,f}^i, \hat{\mathbf{F}}_{k,f}^i, \hat{\mathbf{G}}_{k,f}^i\}$ only for $f \in \tilde{\mathcal{F}}$. For the remaining $f \in \mathcal{F} \setminus \tilde{\mathcal{F}}$, we estimate corresponding matrices using a second-order Lagrange interpolation. For example, given that $\hat{\mathbf{E}}_{k,f_0}^i, \hat{\mathbf{E}}_{k,f_1}^i$, and $\hat{\mathbf{E}}_{k,f_2}^i$ are known at three subcarrier $f_0 < f_1 < f_2$, the value of $\hat{\mathbf{E}}_{k,f}^i$ at any intermediate subcarrier $f \in (f_0, f_2)$ can be approximated as:

$$\hat{\mathbf{E}}_{k,f}^i = l_0 \hat{\mathbf{E}}_{k,f_0}^i + l_1 \hat{\mathbf{E}}_{k,f_1}^i + l_2 \hat{\mathbf{E}}_{k,f_2}^i, \quad (15)$$

where the coefficients are defined as $l_0 = \frac{(f-f_1)(f-f_2)}{(f_0-f_1)(f_0-f_2)}$, $l_1 = \frac{(f-f_0)(f-f_2)}{(f_1-f_0)(f_1-f_2)}$, and $l_2 = \frac{(f-f_0)(f-f_1)}{(f_2-f_0)(f_2-f_1)}$. The same interpolation method also applies to $\hat{\mathbf{F}}_{k,f}^i$ and $\hat{\mathbf{G}}_{k,f}^i$.

2) *The RL Module* : The RL module employ a stochastic policy π_θ to generate compensation matrices $\Delta_{m,n} \triangleq \{\Delta_{m,n}^1, \Delta_{m,n}^2, \dots, \Delta_{m,n}^{I_{max}}\}$ and stopping coefficients $\beta_{m,n} \triangleq \{\beta_{m,n}^1, \beta_{m,n}^2, \dots, \beta_{m,n}^{I_{max}}\}$, where the DU network depth is set as $I_{m,n} = \operatorname{argmax}_i \beta_{m,n}^i$. This design keeps all action vector elements continuous, thereby avoiding the challenges of mixed discrete-continuous optimization. We model the sequential decision-making process of π_θ as a contextual bandit (CB) problem [13] and adopt a model-free RL approach to optimize the policy parameters θ .

Specifically, each downlink block is treated as a single step in the CB setting. The n -th block in the m -th timeslot corresponds to the step $t = mN_b + n$. At each step t , the environment presents a context $s_t \triangleq \{\hat{\mathbf{H}}_{k,f,m,n}^b, \Delta \hat{\mathbf{H}}_{k,f,m,n}^b, \forall k, f\} \in \mathcal{S}$, for which the RL module sample an action \mathbf{a}_t from a Gaussian policy $\pi_\theta(\mathbf{a}_t | s_t)$. The mean and variance of the policy distribution are generated by neural networks $f_{\theta^\mu}(s_t)$ and $f_{\theta^\delta}(s_t)$, respectively, where $\theta \triangleq \{\theta^\mu, \theta^\delta\}$. In response to the action, the environment returns an immediate reward defined as $R(s_t, \mathbf{a}_t) = \hat{\mathcal{R}}_{k,f,m,n} - \hat{\mathcal{R}}_{k,f,m,n}$, where $\hat{\mathcal{R}}_{k,f,m,n}$ and $\hat{\mathcal{R}}_{k,f,m,n}$ denote the EWSR performance of the $I_{m,n}$ -layer RLDDU-Net and the I_{max} -layer DU network without compensation, respectively. Note that shallow depth $I_{m,n}$ may lead to underfitting due to insufficient model capacity, whereas an excessively large $I_{m,n}$ can result in overfitting due to the use of too many compensation matrices. Therefore, the training objective is to optimize the policy such that the expected long-term reward is maximized: $\max_{\theta} \frac{1}{T} \sum_{t=0}^{T-1} \mathbb{E}[R(s_t, \mathbf{a}_t)]$.

Model-free RL is particularly suitable for solving such a CB problem, as it directly optimizes the policy using observed rewards without fitting an explicit reward model. This is especially important here, since the reward function is deeply nested and highly nonlinear, making accurate modeling extremely challenging. Specifically, this paper adopts a stochastic successive convex approximation (SSCA)-based model-free RL algorithm from our prior work [14], which constructs and solves convex surrogate problems, and ensures π_θ convergence to a stationary point of the CB problem. The training code is available at: <https://github.com/kexuanWang-zju/RLDDU-code>. Although it is theoretically possible to train the policy network via unsupervised learning by treating EWSR as the loss function, such methods require first computing the gradient with respect to the action and then backpropagating through the network to update the policy parameters. This nested computation is prone to gradient vanishing, especially in deep architectures. Moreover, in practical systems where parameters such as channel aging coefficients may drift over time, RL enables online adaptation, whereas unsupervised learning methods are typically limited to offline training.

Remark 1. Compared with existing robust precoding algorithms, RLDDU-Net offers three key advantages: 1) RLDDU-Net incorporates domain knowledge from the wideband SWMMSE algorithm, which is theoretically guaranteed to converge to a local optimum of problem \mathbf{P}_1 , thereby achieving more stable performance across diverse scenarios than black-box networks in [8] and [9]; it employs approximation tech-

niques that significantly accelerate convergence and reduce the computational burden of high-dimensional matrix operations and wideband multi-subcarrier processing, outperforming SAA-based and bi-level schemes in [3]–[5]; and it leverages RL-driven design to further enhances its representational capacity over conventional DU schemes with fixed depth and compensation matrices, such as the PO-WMMSE Net in [2].

IV. NUMERICAL RESULTS

We consider a MU-MIMO-OFDM system where a BS with $M_t = 64$ antennas serves $K = \{5, 10, 15, 20\}$ users, each with $M_r = 2$ antennas. Channels are generated using the QuaDRiGa model [15] under the “3GPP_38.901_UMa_NLOS” scenario. Each timeslot lasts 1 ms and is divided in to $N_b + 1 = 7$ blocks. The carrier frequency is 3.5 GHz with a subcarrier spacing of 15 kHz. Users are randomly generated within a 200 m radius around the BS and move at 120 km/h in random directions. The total transmit power is $P = 1$ W. For simplicity, we assume accurate channel estimation at the 0-th block, and that CSI inaccuracies are entirely due to channel aging, characterized by α . Following [2], we statistically obtain $\alpha = \{0.96, 0.92, 0.84, 0.75, 0.63, 0.49\}$ corresponding to the six downlink blocks, where smaller α indicates more severe degradation. For RLDDU-Net, we set the the number of sampled subcarriers frequency-domain interpolation to $\tilde{F} = 8$. The policy networks $f_{\theta^\mu}(\cdot)$ and $f_{\theta^\delta}(\cdot)$ are composed of two convolutional layers (kernel size $H = 3$, channel number $c = 8$, and stride 1) and two fully connected layers (width $d = 128$). Baseline algorithms include wideband the SWMMSE [3], [4] and a wideband extension of PO-WMMSE Net [2] (i.e., perform the PO-WMMSE Net on the central subcarrier to obtain the precoder for the entire RBG), which are referred to as SWMMSE and PO-WMMSE Net for simplicity in the following. All baselines use 5 iterations/layers, while the RLDDU-Net adopts a maximum depth of $I_{max} = 5$. Additionally, since wideband SWMMSE can converges to a local optimum of problem \mathbf{P}_1 with sufficient iterations, we also simulate it with 100-iterations to estimate an upper performance bound.

Fig. 3a illustrates the EWSR performance of algorithms in a scenario with $K = 10$ users and a transmit SNR of 20 dB across various downlink blocks. The results show that SWMMSE, with sufficient iterations (i.e., the estimated upper bound), significantly outperforms WMMSE by accounting for CSI errors. However, with 5 iterations, SWMMSE provides only a marginal improvement over WMMSE due to slower convergence from the SAA method. In contrast, RLDDU-Net far exceeds WMMSE’s performance and approaches the upper bound by directly leveraging CSI statistics (mean and covariance). Simulation statistics reveal that RLDDU-Net requires an average depth of only $\{3.2, 3.2, 3.4, 3.7, 4.1, 4.6\}$ layers across the six blocks, demonstrating superior convergence efficiency. Moreover, RLDDU-Net’s adaptive compensation matrices further enhance performance compared to PO-WMMSE Net. While PO-WMMSE Net, with a fixed compensation matrix, outperforms WMMSE on average, it performs worse than WMMSE in some blocks. RLDDU-Net

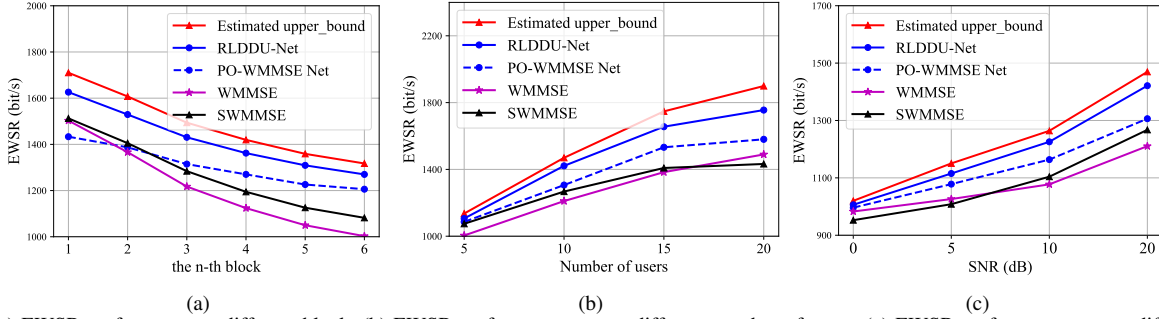


Figure 3. (a) EWSR performance at different block. (b) EWSR performance versus different number of users. (c) EWSR performance versus different SNRs.

Table I
COMPLEXITY COMPARISON

Algorithms	Computational complexity	Values
(S)WMMSE	$O(M_t^2 M_r F K I_{max} + M_t^3 I_{max})$	$2.3e7$
PO-WMMSE Net	$B^2 M_r^2 F K I + q^2 M_r K I + (M_t + q^3) I$	$3e6$
RLDDU-Net	$B^2 M_r^2 \bar{F} K I + q^2 M_r K I + (M_t + q^3) I + (d + C^2) H^2 C B M_r \bar{F} K$	$4e6$

consistently outperforms all other baselines across all blocks, with performance gains becoming more significant in blocks with less accurate CSI. Fig. 3b shows the EWSR performance versus the number of users. As the number of users increases, the EWSR growth rate of all algorithms slows down due to higher interference and the amplified impact of inaccurate CSI. However, the performance gain of RLDDU-Net over the baselines increases, highlighting its superior interference management and robustness. Fig. 3c shows the performance at different SNRs, where RLDDU-Net consistently outperforms the baselines and approaches the estimated upper bound. Moreover, RLDDU-Net shows stronger performance at high SNR compared to the baselines, as performance at high SNR is primarily limited by interference, and RLDDU-Net is more effective at mitigating it.

Finally, we compare the computational complexity of RLDDU-Net with baseline algorithms in Table I, and present numerical results for the typical setup in Fig. 1. RLDDU-Net exhibits comparable computational overhead to PO-WMMSE Net, while significantly reducing complexity compared to conventional WMMSE methods. This is attributed to two key improvements: 1) Its higher convergence efficiency allows for fewer layers compared to the number of iterations required by baseline algorithms, where the average number of iterations of RLDDU-Net is only 3.7 in the simulations; 2) By exploiting beam-domain sparsity (with $B \approx 10$ and $q \approx 30$, both obtained through simulation statistics and smaller than $M_t = 64$) and subcarrier correlation, the matrix computation cost per layer/iteration is greatly reduced, resulting in overall complexity scaling linearly with M_t .

V. CONCLUSION

This paper designs RLDDU-Net for robust WMMSE precoding in massive MU-MIMO-OFDM systems. Derived from wideband SWMMSE, a robust precoding algorithm with theoretical guarantees, RLDDU-Net achieves strong performance under imperfect CSI. By introducing approximation techniques

and leveraging beam-domain sparsity and subcarrier correlation, it greatly reduces computational complexity and accelerates convergence. Additionally, the RL-driven network in RLDDU-Net can adaptively generate compensation matrices to correct approximation errors and adjust network depth. Simulations demonstrate that RLDDU-Net achieves superior throughput with significantly reduced computational burden under imperfect CSI, offering a promising solution for practical WMMSE precoding deployment in real-world systems.

REFERENCES

- [1] Q. Shi, M. Razaviyayn, Z.-Q. Luo, and C. He, "An iteratively weighted MMSE approach to distributed sum-utility maximization for a MIMO interfering broadcast channel," *IEEE Trans. on Signal Process.*, vol. 59, no. 9, pp. 4331–4340, 2011.
- [2] K. Wang and A. Liu, "Robust wmmse-based precoder with practice-oriented design for massive mu-mimo," *IEEE Wirel. Commun. Lett.*, vol. 13, no. 7, pp. 1858–1862, 2024.
- [3] M. Razaviyayn, M. S. Boroujeni, and Z.-Q. Luo, "A stochastic weighted MMSE approach to sum-rate maximization for a MIMO interference channel," in *2013 IEEE 14th Workshop on SPAWC*, 2013, pp. 325–329.
- [4] N. Li, Y. Liu, and L. Zhai, "A robust interference alignment algorithm and the system design," in *2016 11th International Symposium on Antennas, Propagation and EM Theory (ISAPE)*, 2016, pp. 561–564.
- [5] A.-A. Lu, X. Gao, W. Zhong, C. Xiao, and X. Meng, "Robust transmission for massive MIMO downlink with imperfect CSI," *IEEE Trans. on Commun.*, vol. 67, no. 8, pp. 5362–5376, 2019.
- [6] L. You, X. Gao, X.-G. Xia, N. Ma, and Y. Peng, "Pilot reuse for massive MIMO transmission over spatially correlated Rayleigh fading channels," *IEEE Trans. on Wireless Commun.*, vol. 14, no. 6, pp. 3352–3366, 2015.
- [7] J. Shi, W. Wang, X. Yi, X. Gao, and G. Y. Li, "Deep learning-based robust precoding for massive MIMO," *IEEE Trans. on Commun.*, vol. 69, no. 11, pp. 7429–7443, 2021.
- [8] H. Sun, X. Chen, Q. Shi, M. Hong, X. Fu, and N. D. Sidiropoulos, "Learning to optimize: Training deep neural networks for interference management," *IEEE Trans. Signal Process.*, vol. 66, no. 20, pp. 5438–5453, 2018.
- [9] W. Lee, M. Kim, and D.-H. Cho, "Deep power control: Transmit power control scheme based on convolutional neural network," *IEEE Commun. Lett.*, vol. 22, no. 6, pp. 1276–1279, 2018.
- [10] Q. Xu, J. Sun, and Z. Xu, "Robust frequency selective precoding for downlink massive mimo in 5g broadband system," *IEEE Trans. Veh. Technol.*, vol. 72, no. 12, pp. 15941–15952, 2023.
- [11] A. Liu, L. Lian, V. K. N. Lau, and X. Yuan, "Downlink channel estimation in multiuser massive MIMO with hidden Markovian sparsity," *IEEE Trans. on Signal Process.*, vol. 66, no. 18, pp. 4796–4810, 2018.
- [12] D. Tylavsky and G. Sohie, "Generalization of the matrix inversion lemma," *Proceedings of the IEEE*, vol. 74, no. 7, pp. 1050–1052, 1986.
- [13] R. S. Sutton, A. G. Barto *et al.*, *Reinforcement learning: An introduction*. MIT press Cambridge, 1998, vol. 1, no. 1.
- [14] L. Zhang, A. Liu, and K. Wang, "A hybrid reinforcement learning framework for hard latency constrained resource scheduling," *arXiv preprint arXiv:2504.03721*, 2025.
- [15] J. Shi, A.-A. Lu, W. Zhong, X. Gao, and G. Y. Li, "Robust wmmse precoder with deep learning design for massive MIMO," *IEEE Trans. on Commun.*, 2023.